

Physics-Based Causal Reasoning for Safe & Robust Next-Best Action Selection in Robot Manipulation Tasks

Ricardo Cannizzaro¹, Michael Groom¹, Jonathan Routley¹, Robert Ness², and Lars Kunze¹

Abstract—Safe and efficient object manipulation is a key enabler of many real-world robot applications. However, this is challenging because robot operation must be robust to a range of sensor and actuator uncertainties. In this paper, we present a physics-informed causal-inference-based framework for a robot to probabilistically reason about candidate actions in a block stacking task in a partially observable setting. We integrate a physics-based simulation of the rigid-body system dynamics with a causal Bayesian network (CBN) formulation to define a causal generative probabilistic model of the robot decision-making process. Using simulation-based Monte Carlo experiments, we demonstrate our framework’s ability to successfully: (1) predict block tower stability with high accuracy (Pred Acc: 88.6%); and, (2) select an approximate next-best action for the block stacking task, for execution by an integrated robot system, achieving 94.2% task success rate. We also demonstrate our framework’s suitability for real-world robot systems by demonstrating successful task executions with a domestic support robot, with perception and manipulation sub-system integration. Hence, we show that by embedding physics-based causal reasoning into robots’ decision-making processes, we can make robot task execution safer, more reliable, and more robust to various types of uncertainty.

I. INTRODUCTION

Safe and efficient object manipulation is vital to many real-world robot applications. The way in which objects are manipulated can have a significant impact on both task performance and safety. Further, robot operation must be robust to the different sources of uncertainty — i.e., stochastic action outcomes, and partial and noisy sensor observations — that they are subjected to in the real world [1]. By reasoning about the physical consequences of robot manipulation actions before committing to them, undesirable and unsafe outcomes can be avoided.

In this paper, we present a physics-informed causal inference framework to allow a robot to probabilistically reason about its object placement actions in a block stacking task. We integrate a physics-based simulation with a causal Bayesian network (CBN) formulation to define a causal generative probabilistic model of the robot decision-making process. We conduct Monte Carlo experiments in simulation to validate the proposed framework’s ability to accurately predict block tower stability and reliably select the next-best action for the block stacking task, executed by an integrated robot system equipped with perception and manipulation sub-systems. Further, we conduct a robot hardware

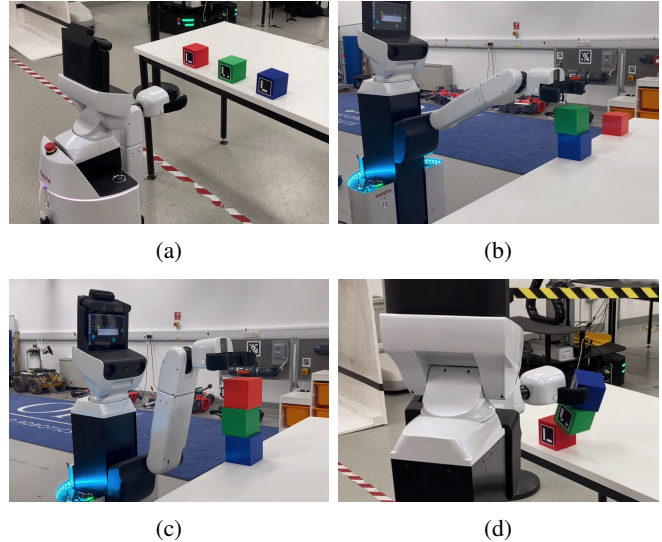


Fig. 1: An illustration of a two-action block stacking task and possible success/failure outcomes. (a) Initial task state: three blocks are laid out on the table. (b) Intermediate task state: two blocks form a partially-built stable tower. (c) Task success: all blocks are placed into a stable tower. (d) Task failure: improper block placement causes the tower to topple.

demonstration of our framework, showing the transferability and robustness of it to real-world robot systems. Thus, we show that by embedding this type of reasoning into robots’ decision-making, they can achieve more reliable, safe, and effective performance.

The main contributions of our paper are as follows:

- 1) A novel physics-informed CBN-based causal generative probabilistic model to formally describe a robot agent undertaking a block stacking task with stochastic actions in a partially observable environment;
- 2) A novel task reasoning framework that uses association- and intervention-based causal inference to predict block tower stability and find a greedy next-best action solution for block placement;
- 3) A simulation-based experimental validation of an integrated mobile robot system performing block stacking tasks, using the proposed decision-making framework;
- 4) A robot hardware demonstration of our framework.

We provide an overview of existing literature in Section II, formally define the manipulation problem in Section III, and present causal machine learning preliminaries in IV. Then in Section V, we provide an overview of our proposed CBN-based causal model formulation, sensor and actuator noise characterisation process, and our proposed causal reasoning

¹Oxford Robotics Institute, Dept. Engineering Science, University of Oxford, UK. Correspondence email: ricardo@robots.ox.ac.uk

²Microsoft Research, Redmond, WA, USA

This work is supported by the Australian Defence Science & Technology Group and the EPSRC RAILS project (grant reference: EP/W011344/1).

framework for robot manipulation tasks. In Section VI, we describe our simulation-based experimental validation, and present and discuss results in Section VII. Finally, in Section VIII we present a real-world demonstration of the block stacking task using a fully-integrated mobile robot system.

II. RELATED WORK

Robot manipulation is a long-standing field of research that seeks to address control problems that require consideration of contact forces between an object and a robot end-effector, and the joint motion of the two towards an end goal configuration. This covers a wide range of tasks including construction, assembly, pick-and-place, insertion, and peg-in-hole tasks [2]–[6].

A. Causality in Robot Manipulation

A growing list of recent works in the literature have identified causality as a vital component of trustworthy autonomous robot systems [7]–[10], possessing the potential to address current limitations of machine learning approaches such as domain transfer issues [11], and be a vital tool to realise the desirable properties of explainability, fairness, and accountability [7] — characteristics typically not achievable with “black-box” deep learning methods.

Despite this, research has only recently begun to consider causality for robot manipulation tasks at a *semantic* level [12]–[15]. In recent work by Diehl & Ramirez-Amaro [13], the authors formulate the block stacking task as a CBN. They learn task success probabilities offline from data collected through physics-based simulations of task outcomes given action parameterisation, and then demonstrate prediction and action selection using the learned model. However, the model does not include the number of blocks and their physical attributes (e.g., dimensions, mass), and is fixed after training. Thus, any change in the task in terms of the number of blocks and/or the block attributes necessitates the retraining of the model. Further, sensor noise or manipulation error of the robot are not explicitly included as random variables in their model formulation, and thus the model contains implicitly-learned data-driven assumptions that limits the re-use of the model for different robot platforms. In follow-up work, the authors use a CBN model to explain, predict, and prevent failures in block stacking tasks [14]. However, the CBN is again fixed after training on simulation-based task execution data and does not include the number of blocks and their physical attributes. Thus, their method cannot be used to solve block stacking tasks with more generalised definitions.

Other recent efforts to address robot manipulation with causality include *CausalWorld* [15], which provides a benchmark for causal structure and transfer learning in a physics-based simulation environment. Although the physical attributes are explicitly included in their modelling, the focus of this work is to provide a tool to reinforcement learning researchers that gives fine-grained control over how varied task distributions are during the generation of manipulation datasets, to be used for learning policies via transfer learning — rather than providing a physics-based simulation tool

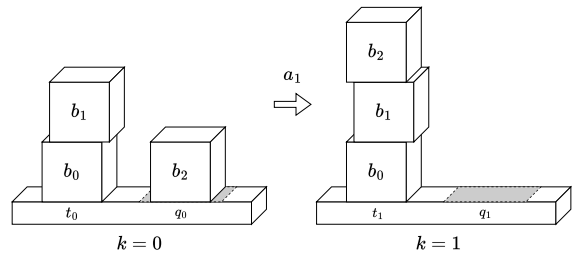


Fig. 2: The robot block stacking problem considered in our work. At each time step k the robot must select a position in which to place the next block b from the queue q into the tower t , such that the tower remains stable after the block placement action a is performed. This continues until all blocks in the queue have been placed.

that can be directly used to learn effective policies for manipulation tasks online.

The recent increase in maturity and flexibility of probabilistic programming languages (PPLs) such as Pyro [16] has recently unlocked the implementation of causal models as probabilistic programs. As shown in our past work [17], a Pyro-based CBN model formulation can be easily upgraded into a Pyro-based Structural Causal Model (SCM) [18], a strictly more expressive class of causal model that permits counterfactual inference, which is necessary for the generation of causal explanations that are aligned with human causal judgements [19], proposed as a vital tool for building safe, reliable, explainable, and trustworthy autonomous systems [20], [21]. Therefore, this presents an opportunity to extend a Pyro-based CBN model — such as the one we propose for the block stacking task — to an SCM-based formulation, and thus unlock the ability generate counterfactual-based causal explanations for what the robot has seen and done during its task execution.

Other recent works also explore physics-based reasoning about physical properties of the world, including stability — however, they do so without the causal semantics required for the causal analysis of the manipulation tasks [22]–[24]

III. PROBLEM DEFINITION AND NOTATION

In the sequential block stacking task considered here (Figures 1 and 2), the robot’s task is to incrementally build a tower starting from a specified initial state and ordered list of blocks to be placed, relying on sensor observations.

More formally, we label each block state b_n with a subscript $n \in \mathbb{N}$, $n < N$, indicating its intended place in the N -length final tower, and each state s_k with its corresponding time step $k \in \mathbb{N}$, $k \leq K$, in the K -action task episode.

The robot’s task is to build a tower starting from an initial state s_0 , consisting of an ordered set of one or more blocks of initial length N_{Init} , $\mathbf{b}_0 = [b_0, b_1, \dots, b_{N_{Init}-1}]$, by adding a defined sequence of blocks $\mathbf{q} = [b_{N_{Init}}, \dots, b_{N-1}]$, each with specified mass and dimensions, over K time steps to create a stable final tower with state s_K that remains standing without any external support.

The task is considered a failure if the tower falls at any point, and a success if the tower remains standing after the final block placement. A key challenge is the presence of noise in sensor measurements and errors in the state estimation and control modules; these uncertainties must be considered for robots to complete the task reliably.

To simplify the task at hand, we consider only single-column towers in our work. Consequently, to exploit the independence of actions in this sequential-action task, we constrain the task to solving a sequence of independent next-best action-selection problems. Further, we consider the task being undertaken in a partially-observable environment, in which the robot does not have access to the underlying world state S_k but instead must rely on noisy observations Z_k from its sensors. At each time step k , we formulate the next-best block placement problem as finding the optimal action \hat{a}_k from the set of actions available to the robot \mathcal{A} , parameterised by block placement position $a = (x, y)$ on top of the current top block, that maximises the probability of the resultant tower S_k being stable, given the noisy observation Z_{k-1} of the hidden previous tower state S_{k-1} :

$$\hat{a}_k = \underset{a_i \in \mathcal{A}}{\operatorname{argmax}} \{P(\text{IsStable}(S_k) \mid Z_{k-1}, A_k = a_i)\}.$$

IV. BACKGROUND

Causality is the science of reasoning about cause and effect [25]. In causal machine learning, causal models encode the causal relationships that describe the data-generation process of a system. These relationships are strictly causal, rather than being merely association-based.

CBNs are a type of generative causal probabilistic graphical model used in causal modelling and inference [18], in which causal relationships are represented by an underlying causal directed acyclic graph (DAG) (Figure 3). A causal DAG G is defined as $G = \langle V, E \rangle$, where V is the set of nodes, representing random variables in the causal model, and E is the set of directed edges, the presence of which between two variables denoting the existence of a conditional dependency of the child on the parent node. A CBN is fully specified by a causal DAG and a set of causal Markov kernels $P(v_i | pa(v_i)) \forall v_i \in V$, where $pa(\cdot)$ is the set of direct parents in the causal graph. As such, CBNs encode a joint probability over the random variables in the model. Crucially, the causal semantics of CBNs allow us to reason about how an *intervention*, taken on the system to interrupt the natural causal relationship that governs the data-generation process in one variable X , should change our belief in another Y : $P(Y | do(X = x))$. Here, the $do(\cdot)$ operator defines an intervention to modify a variable outcome in the model [18].

V. METHOD FOR PHYSICS-BASED CAUSAL REASONING

A. CBN Robot-Task-World Model Definition

1) *Modelling the Data-Generation Process*: We model the data-generation process of the robot-task system as a CBN-based sequential action selection problem. The underlying causal DAG describes the robot’s decision-making process and the system dynamics for a K -action block stacking task.

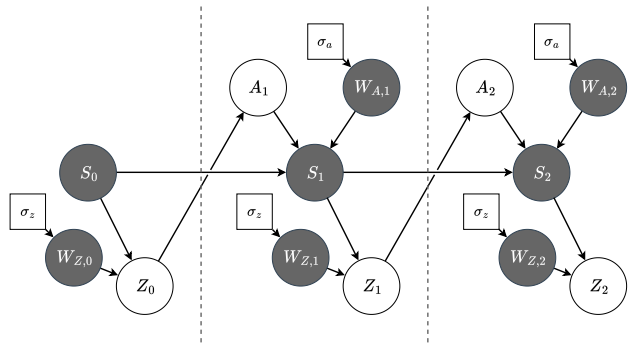


Fig. 3: The causal DAG used in the CBN-based model formulation, describing the robot’s decision-making process and the system dynamics for a two-action ($K = 2$) block stacking task. At each time step k , based on its *observation* of the previous tower state Z_{k-1} the robot selects a stochastic action A_k to take (with random noise $W_{A,k}$) to transition the current hidden ground truth tower state from S_{k-1} to S_k , and then obtains a noisy measurement Z_k of the updated state (with random noise $W_{Z,k}$). The task is considered a success if the final tower state S_N is stable, otherwise failure. Observed variables are shown as white circular nodes, unobserved as grey. Square nodes indicate model parameters.

An unrolled causal DAG for a two-action ($K = 2$) block stacking task is illustrated in Fig. 3.

Crucially, our model captures two main sources of (unavoidable) uncertainty in the robot-task system: the random observation noise $W_{z,k}$ and the actuation noise $W_{a,k}$ at each time step k . The ground truth state S_k is not available to the robot, instead it must rely on its noisy observation from the environment Z_k . Further, due to imperfect control and state estimation of the mobile robot system, the execution of a chosen action A_k does not lead to a deterministic outcome, rather it is perturbed by a random error term $W_{A,k}$, which captures the error in block placement due to the propagation of various perception, state estimation, and actuation errors.

2) *Task State Representation*: We model the state of each block b by tracking its physics-related properties — i.e., position, dimensions, and mass. We model the tower state t_k at time k as a list of block states of size N_k , ordered in ascending height: $t = [b_0, b_1, \dots, b_{N-1}]$ (we omit the time index k here for readability). We re-iterate that each block is labelled with n , indicating its intended position in the final tower, and note that this does not necessarily correspond to the time step index k at which it is placed. Finally, we model the block stacking task state s_k by augmenting the tower state t_k with the queue (i.e., ordered list) of blocks remaining to be placed into the tower q_k : $s_k = t_k \cup q_k$.

We note that the robot state is absent from our task state abstraction. This is because we assume that the robot-task-world causal system is independent of the robot state, i.e., is only conditional on the task state and robot *action*.

3) *Action Representation*: We parameterise each action in the robot action set $a \in \mathcal{A}$ as $a = (x, y)$, representing the intended 2D position of placement of the next block, in the local coordinate frame defined by the centre of the top face

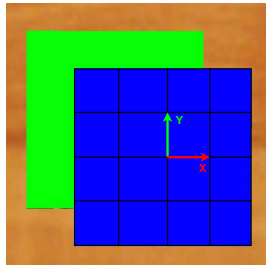


Fig. 4: A top-down view of a block tower illustrating how the candidate action positions (x, y) are uniformly sampled from a grid spanning the top of the current top block (blue), in the local coordinate frame located at the face centre.

of the current top block, aligned with its orientation as shown in Figure 4. The height of the next block is always chosen such that it is placed on the top surface of the previous block, and thus is omitted from the action representation.

4) *Transition Function Representation*: We model our state transition function T in the standard (PO)MDP formulation. However, we represent the agent’s action choice as an intervention, using the $do(\cdot)$ operator instead of a condition statement; we also include the action error term $W_{A,k}$:

$$T(S, A, S') = P(S_k | S_{k-1}, do(A_k = a_k), W_{A,k}).$$

To compute the value of s_k that is sampled from the transition function T , we use the PyBullet 3D physics simulator [26] to simulate the full-system rigid body dynamics of the block tower (Figure 5), based on the agent’s observation.

The simulator is used to forward-simulate the evolution of the physical system, from the time at which the block is placed onto the tower (i.e., after being released by the robot), until either a testing period has elapsed, or the time at which the block and/or tower have been detected to have fallen, whichever is sooner. Upon terminating the forward-simulation, the final state of the block tower in the PyBullet simulation is assigned to the sampled value of s_k .

5) *Noise & Error Modelling*: We model observation noise as a random variable drawn from a zero-mean isotropic 3D Gaussian distribution with a single shared standard deviation of σ_z . This parameter represents the magnitude of additive noise present in the robot system’s block position measurement due to perception and estimation errors, assumed to be independent in each of the x-, y-, and z-axes.

Similarly, we model manipulation noise as a random variable drawn from a zero-mean isotropic 3D Gaussian distribution with a single shared standard deviation of σ_a . This parameter represents the magnitude of additive noise present in the robot system’s block placement action due to control and state estimation errors, also assumed to be independent in each of the x-, y-, and z-axes.

B. Task 1: Tower Stability Prediction

In our proposed framework, we frame the tower stability prediction task as a binary classification problem and seek to infer the probability that an observed tower configuration will remain standing. More formally, we estimate the association-based inference query $\Phi_{stable,k}$ using our robot-task-world

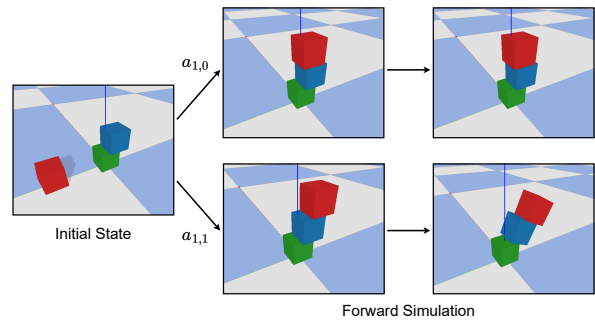


Fig. 5: Physics-based PyBullet simulations used to assess candidate actions during the next-best action selection process, accounting for sensor and manipulation errors.

causal model to estimate the probability the tower state S_k is stable, conditional on the robot’s noisy observation z_k :

$$\Phi_{stable,k} = P(IsStable(S_k) = True | Z_k = z_k, W_{Z,k}),$$

and apply a threshold value $\tau_{stable,Z}$ for binary classification:

$$\hat{y}_k = True \text{ iff } \Phi_{stable,k} \geq \tau_{stable,Z}.$$

The stability threshold $\tau_{stable,Z}$ acts as a tuning parameter, which defines the tolerance for acceptable uncertainty in the prediction, due to block position measurement error. Intuitively, we anticipate this threshold should be set higher for robot systems with higher perception noise, to reduce the number of false positive (i.e., stable) classifications. We expect the opposite for systems with lower perception noise; i.e., the threshold can be set lower to reduce the number of false negatives while avoiding an increase in false positives.

We note that in the context of the tower stability classification being used for downstream tasks such as tower construction (Section V-C) or safety fault detection, it is typically more important to minimise the false positive rate since, depending on the application, the consequences of miss-classifying an unstable tower may potentially be much greater than miss-classifying a stable tower. For example, more conservative classification would be beneficial if stacking objects that may break if they were to fall, or cause harm/damage to nearby humans or equipment.

C. Task 2: Next-Best Action Selection

In our framework, we frame the next-best action selection task as an optimisation problem and seek to find the action parameterisation that maximises the predicted probability of the resultant tower remaining standing after block placement.

To begin, we generate candidate action position parameterisations $a_i = (x_i, y_i)$ by uniformly sampling positions from a $L \times W$ grid spanning the top face of the current top block, with positions being relative to the local block-aligned coordinate frame located at the face centre (Figure 4).

For each candidate action, we calculate the intervention-based inference query $\Phi_{stable,k+1,a}$ using our CBN model, to estimate the probability of the resultant tower state S_{k+1} being stable, conditioned on the noisy observation z_k and

taking an **intervention** to set the selected action A_{k+1} to the candidate action a_i using the $do(\cdot)$ operator:

$$P \left(\begin{array}{l} \text{IsStable}(S_{k+1}) = \text{True} \mid \dots \\ do(A_{k+1} = a_i), Z_k = z_k, W_{Z,k}, W_{A,k} \end{array} \right)$$

We apply a threshold value $\tau_{stable,A}$ to filter out action candidates with stability probabilities below an acceptable threshold. We then find the action with the highest probability $a^* = \operatorname{argmax}_{a_i \in \mathcal{A}} P(\text{Stable}|do(a_i))$ and apply clustering to define the *stable set* of actions \mathcal{A}_{stable} with probabilities within distance $\tau_{cluster}$ of the highest probability p_{a^*} :

$$\mathcal{A}_{stable} = \{a_i \in \mathcal{A}, \text{ s.t. } |p_{a^*} - p_{a_i}| \leq \tau_{cluster} \text{ and } p_{a_i} \geq \tau_{stable,A}\}.$$

We assume that the stable set \mathcal{A}_{stable} forms a convex hull approximating the block placement region of stability, and find the centroid of this region by computing the geometric mean of the (x, y) positions of the actions in the stable set. This centroid is selected as the next-best action a_k .

The post-placement stability threshold $\tau_{stable,A}$ acts as a tuning parameter, which defines the tolerance for acceptable uncertainty in the action success, due to block position measurement error and block placement error. The cluster threshold $\tau_{cluster}$ acts as a second tuning parameter, which defines how close the stable actions need to be to the highest probability action in order to be included in the geometric mean operation. Similar to $\tau_{stable,Z}$, these thresholds should be tuned to the application requirements — i.e., made more conservative for higher-risk applications.

VI. EXPERIMENTATION

A. Gazebo Robot Simulation

We evaluate the performance of our framework by performing Monte Carlo experiments using a simulated Toyota Human Support Robot [27] and blocks in the Gazebo simulation environment [28]. Three 7.5cm-long cube-shaped blocks are used in experiments. To simulate a realistic block position estimation system, we attach ArUco markers to each block and use simulated RGB-D sensor data as an input to the OpenCV ArUco marker pose estimation module [29] to generate observations of block pose. To simulate realistic robot manipulation, we use ROS MoveIt! [30] to generate and execute robot pick-and-place motion plans.

B. Task 1: Tower Stability Prediction

In this section we describe the experimental validation of our model’s ability to predict the stability of existing block tower configurations, based on the robot’s noisy observations.

1) *Block Pose Estimation Error Model Characterisation:* We generate a training dataset of 250 randomly-generated 3-block tower configurations for characterising the error present in the robot’s block position estimation in Gazebo simulation. For each tower configuration, we record the 3D positions of each block as observed by the robot and the ground truth block positions in the simulation world. The block position estimation error is characterised by calculating

the position error for all tower configurations, then calculating the standard deviation $\sigma_{pos,x}$, $\sigma_{pos,y}$ and $\sigma_{pos,z}$ along each axis. Finally, we take the observation noise standard deviation σ_z as the average of these three values.

2) *Tower Stability Classification Accuracy:* We generate in simulation a testing dataset of 1000 randomly generated 3-block towers to test our model’s classification accuracy. Ground truth labels are generated by forward-simulating tower configurations in the Gazebo physics-based simulation and observing whether they remained standing. We use the Importance Sampling inference implementation in Pyro, with 50 samples, to infer tower stability probabilities and thus make binary tower stability classifications using the defined stability probability threshold. To evaluate the predictive performance of our model, we compute conventional classification metrics — F1 score, AUC score, precision, and recall — over a range of stability thresholds.

C. Task 2: Next-Best Action Selection

In this section we discuss the experimental validation of our model’s ability to select the next-best action for where to place the next block, in a greedy manner. In our evaluation, we specifically consider placing one block ($K = 1$) onto block towers of initial length two ($N = 2$).

1) *Block Placement Error Model Characterisation:* Here, we describe our method used to characterise the error present in the robot’s block placement using the manipulation subsystem. We generate a training dataset of 25 randomly-generated 2-block tower configurations, used to define the initial tower state in the Gazebo simulation world. The robot performs 10 independent attempts to place one additional block at a predefined position. This produces a total of 250 experiments. After each robot placement attempt, the placement position error (i.e., deviation from intended place position) is measured. From these position error measurements, we calculate the standard deviations used to characterise the 3D block placement errors: $\sigma_{pos,x}$, $\sigma_{pos,y}$ and $\sigma_{pos,z}$. Finally, we take the manipulation noise standard deviation σ_a as the average of these values.

2) *Next-Best Action Selection Performance:* To test our system’s performance on the next-best action selection task in simulation, we generated a test dataset of 50 randomly generated initial 2-block tower configurations. We use our next-best action selection method for each tower configuration to select the position to place one additional block into the tower (i.e., a single-action task, $K = 1$). For each selected action, we attempt the block placement independently 10 times with the simulated robot system, for a total of 500 experiments. To evaluate task performance, the tower stability is recorded shortly after the block is placed by the simulated robot. A placement action is considered successful if the resultant tower remains stable.

We sample candidate action positions from a 5×5 grid spanning the top face of the current top block. Inference is performed using the Importance Sampling inference implementation in Pyro with 50 samples, to infer tower stability probabilities at each candidate position.

For the causal-inference-based next-best action selection method, we set the post-placement stability threshold $\tau_{stable,A} = 0.80$ to ensure we have high certainty that the selected action results in a stable tower. We use the clustering threshold $\tau_{cluster} = 0.20$, to accept all candidates with probabilities above the post-placement stability threshold into the stable set, to demonstrate more clearly the benefits of the final centroid-based selection process.

To control for extraneous effects caused by failures associated with robot sub-systems not considered in this evaluation (e.g., robot base control, sample-based motion planning), we implement a simulation experiment supervisor program to detect failures outside of the scope of this evaluation and trigger a reset of the simulated experiment episode.

3) *Naive Baseline Action-Selection Method*: We evaluate the performance of our method against a baseline method that uses a naive heuristic-based hand-crafted policy, which selects the centre of the current top block as the next action — a heuristic that can reasonably be expected to lead to the construction of stable towers most of the time.

VII. RESULTS & DISCUSSION

A. Task 1: Tower Stability Prediction

1) *Quantitative Results*: Our model’s prediction performance on the testing block tower dataset is shown in Table I and Figure 6. The best stability threshold was found to be 0.4 based on the Youden’s index from the ROC curve, corresponding to a precision of 0.955 and recall of 0.868. Motivated by reasons discussed earlier in Section V-B, this optimal threshold was selected because it yielded a lower false positive rate than the precision-recall curve optimal threshold (calculated from F1-score). These values are very close to the ideal classification performance, and thus demonstrate a strong predictive ability of our model.

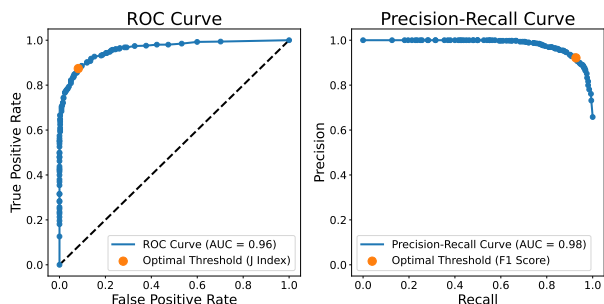


Fig. 6: Receiver operating characteristic (ROC) and precision-recall curve plots based on model predictions of tower stability. These curves are very close to ideal performance, indicating very strong model classification performance. The optimal threshold is taken using Youden’s Index.

Sensor Model Characterisation - Results from the block position measurement error characterisation are listed in Table II. Measurement errors are illustrated in Figure 7, which shows the block position measurement error distribution, in the Gazebo simulation world frame. The plot shows that our

Metric	Score (\uparrow)
Prediction Accuracy	88.6%
F1-Score	0.909
Precision	0.955
Recall	0.868
AUC Score	0.961

TABLE I: Prediction Results: The model achieves strong classification performance, very close to ideal classification. assumption that the random error term W_Z is independent of robot state does not hold because the error distribution in the X-axis, corresponding roughly to the depth axis of the robot’s camera, exhibits a non-zero error distribution with a significantly larger standard deviation than the other axes. Regardless, we continue forward with the assumption that these epistemic modelling errors do not contribute significantly to model performance. As shown in Table II, we take $\sigma_z = 0.469cm$ as our block position sensor measurement scale parameter for the Gaussian error distribution.

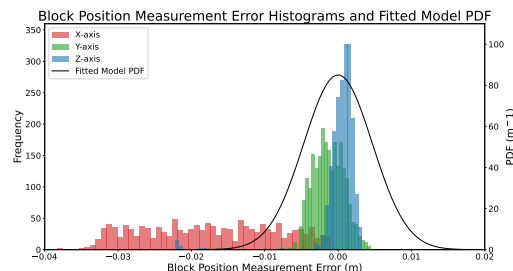


Fig. 7: Block Position Measurement Error Characterisation: Histograms of block position measurement errors along the X-, Y-, and Z-axes, with the modelled probability density function (PDF), fitted from the training dataset, overlaid.

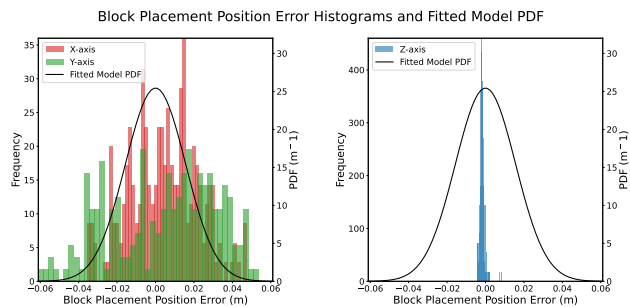


Fig. 8: Block Placement Position Error Characterisation: Side-by-side histograms illustrating block placement position errors on the X- and Y-axes (left) and the Z-axis (right), each with the modelled probability density function (PDF), fitted from the training dataset, overlaid.

B. Task 2: Next-Best Action Selection

1) *Quantitative Results*: **Manipulation Model Characterisation** - Due to Gazebo simulation errors, only 211 out of the total 250 placement attempt experiments yielded measurements that could be used for placement error characterisation. These errors did not impact the remaining measurements used to characterise the placement error. Figure

	Measurement Error (cm)	Placement Error (cm)
$\sigma_{pos,x}$	0.906	1.79
$\sigma_{pos,y}$	0.216	2.77
$\sigma_{pos,z}$	0.284	0.146
$\sigma_{z/a}$ (avg.)	0.469	1.57

TABLE II: Block Position Measurement and Placement Error Characterisation: The standard deviations of position measurement error and placement position error; for x, y, and z global frame axes; learned from the simulation training data. The model parameters σ_z and σ_a are taken as the average of the three axes standard deviations for measurement and position respectively.

Action-Selection Method	Number of Task Successes	Number of Task Failures	Task Success Rate
Baseline	372	128	74.4%
Causal (Ours)	471	29	94.2%
Baseline - Ideal	35	15	70.0%
Causal (Ours) - Ideal	50	0	100%

TABLE III: Block stacking performance with a simulated robot system: Our causal-inference based action-selection method achieves a stronger task success performance than the baseline method (\uparrow **19.8%**), likely due to explicitly accounting for block rigid-body physics and uncertain sensing and manipulation. Our method again performs stronger in the ideal case, in which there is no manipulation error (\uparrow **30%**).

8 shows the block placement position error distributions. Similar to Figure 7, it is shown that the block placement errors in the X and Y axes have a much larger standard deviation than the Z axis. This is likely caused by much higher uncertainty in the robot state estimation in these axes. Again, we make the assumption that modelling errors do not contribute significantly to model performance and take $\sigma_a = 1.57cm$ as our block position sensor measurement scale parameter for the Gaussian error distribution.

Simulated Robot System Task Evaluation - Results of the next-best action selection evaluation using the simulated robot system are presented in Table III. Our causal-inference based action-selection method achieves a stronger task success performance than the baseline, **up 19.8 percentage points**. Our method also performs stronger in the ideal case, i.e., with no manipulation error, **up 30 percentage points**.

Figure 9 provides an exemplar heatmap visualisation of predicted probabilities of stability for candidate placement positions, used to inform next best action decision-making during task execution, accounting for both perception and manipulation errors, for a robot system with low and high system uncertainties, for a particular initial tower state.

2) *Qualitative Results*: The increased performance of our causal-inference-based method over the baseline method is likely due to it explicitly accounting for the block rigid-body physics and the uncertainties introduced by sensor noise and manipulation error.

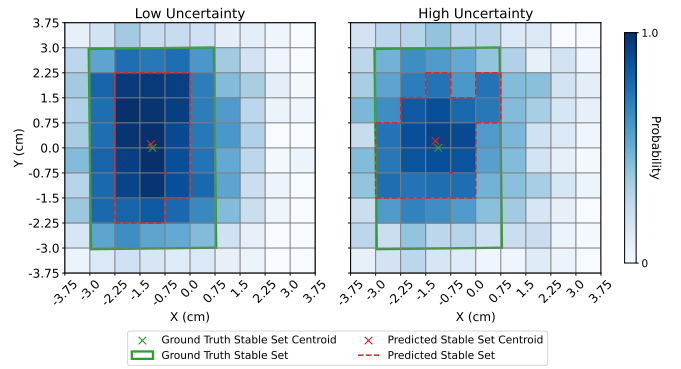


Fig. 9: Heatmap visualisation of predicted probabilities of stability for candidate placement positions (sampled across the current top block face), accounting for perception and manipulation errors, for a robot system with low (LHS) and high (RHS) system uncertainties, for a particular initial tower state and stability threshold of 0.8. The predicted stable set and its centroid (selected as the robot’s final choice) is shown in red; ground truth stability region and associated centroid (determined via Gazebo simulation) in green. The increased uncertainty causes a decrease in stability probability close to the edge of the ground truth stable region, where the random errors in perception and manipulation have a greater chance of making the resultant tower unstable.

First, through the use of the PyBullet 3D physics simulation environment, our method is able to perform realistic and highly accurate simulations of the full system dynamics and thus accurately predict the stability of individual candidate block tower configurations. Because these mental simulations are used to inform the online action-selection process, our method’s decision making is highly robust to precarious initial configurations (e.g., one of the intermediate blocks being placed off-centre). This is demonstrated by our method performing perfectly across the 50 ideal block stacking tasks (i.e., no manipulation error).

Second, since the random block position estimation error and block placement errors are explicitly modelled in our model formulation, we are able to take a probabilistic approach to decision-making under uncertainty. This likely makes our framework more robust to the sources of uncertainty robot systems are typically subjected to, and thus more likely to have a better performance than other approaches that do not account for these uncertainties.

Conversely, the baseline method is a static policy, which does not take into account the full system dynamics, instead relying on a simple heuristic which can not be expected to generalise well to all tower configurations. Our experiments demonstrate using the baseline method is more likely to lead to task failure outcomes for precarious initial tower configurations from our testing dataset while using our method is more likely to lead to task success outcomes.

VIII. REAL-WORLD HUMAN SUPPORT ROBOT DEMONSTRATION

We demonstrate the execution of a 2-action block stacking task, starting with an initial 1-block tower state on a real-

world Toyota Human Support Robot to validate its suitability for real-world robot manipulation tasks (Figure 1). Except for being a more difficult task, the real-world robot demonstration setup is an almost exact recreation of the simulated 1-action task experiment setup. No parameter re-tuning is performed for any component of the robot system.

We performed 5 attempts of the 2-action stacking task and observed 4 successful attempts and 1 unsuccessful attempt (80% success rate). This result demonstrates our method's suitability for real-world block stacking tasks and ability to transfer from simulation to real robot systems — requiring zero system modification or re-tuning, or model retraining.

IX. CONCLUSION

We present a physics-informed causal-inference-based framework for a robot to probabilistically reason about candidate actions in a block stacking task, integrating a physics-based simulation of the rigid-body system dynamics with a CBN-based formulation of the next-best action problem. Through simulation-based experimental validation, we demonstrate that our model is able to very accurately predict block tower stability with 88.6% accuracy, and also find an approximately next-best action for execution by an integrated robot system that achieves 94.2% task success rate. We also demonstrate our method to be successful on real-world task executions, thus demonstrating the suitability of our method for real-world robots. This work demonstrates how causal reasoning methods can be combined with physics-based simulators to unlock benefits for robot manipulation decision-making under uncertainty, and opens up the path to vital future research on post-hoc counterfactual-based explanation methods for trustworthy autonomous robot systems.

REFERENCES

- [1] H. Kurniawati, "Partially observable markov decision processes and robotics," *Annual Review of Control, Robotics, and Autonomous Systems*, vol. 5, no. 1, pp. 253–277, 2022.
- [2] M. Suomalainen, Y. Karayiannidis, and V. Kyrki, "A survey of robot manipulation in contact," *Robotics and Autonomous Systems*, vol. 156, p. 104224, 2022.
- [3] J. Collins, M. Robson, J. Yamada, M. Sridharan, K. Janik, and I. Posner, "Ramp: A benchmark for evaluating robotic assembly manipulation and planning," 2023.
- [4] J. Yamada, J. Collins, and I. Posner, "Efficient skill acquisition for complex manipulation tasks in obstructed environments," 2023.
- [5] S. Gubbi, S. Kolathaya, and B. Amrutur, "Imitation learning for high precision peg-in-hole tasks," in *2020 6th International Conference on Control, Automation and Robotics (ICCAR)*, pp. 368–372, IEEE, 2020.
- [6] J. Luo, O. Sushkov, R. Pevceviciute, W. Lian, C. Su, M. Vecerik, N. Ye, S. Schaal, and J. Scholz, "Robust multi-modal policies for industrial assembly via reinforcement learning and demonstrations: A large-scale study," 2021.
- [7] N. Ganguly, D. Fazlija, M. Badar, M. Fisichella, S. Sikdar, J. Schrader, J. Wallat, K. Rudra, M. Koubarakis, G. K. Patro, W. Z. E. Amri, and W. Nejdl, "A review of the role of causality in developing trustworthy ai systems," 2023.
- [8] T. Hellström, "The relevance of causation in robotics: A review, categorization, and analysis," *Paladyn, Journal of Behavioral Robotics*, vol. 12, pp. 238–255, 2021.
- [9] B. M. Lake, T. D. Ullman, J. B. Tenenbaum, and S. J. Gershman, "Building machines that learn and think like people," *Behavioral and Brain Sciences*, vol. 40, p. e253, 11 2017.

- [10] L. Castri, G. Beraldo, S. Mghames, M. Hanheide, and N. Bellotto, "Ros-causal: A ros-based causal analysis framework for human-robot interaction applications," in *Causal-HRI: Causal Learning for Human-Robot Interaction* workshop at the 2024 ACM/IEEE International Conference on Human-Robot Interaction (HRI), March 2024.
- [11] J. Pearl, "The seven tools of causal inference, with reflections on machine learning," *Commun. ACM*, vol. 62, pp. 54–60, 2 2019.
- [12] C. Uhde, N. Berberich, K. Ramirez-Amaro, and G. Cheng, "The robot as scientist: Using mental simulation to test causal hypotheses extracted from human activities in virtual reality," pp. 8081–8086, 2020.
- [13] M. Diehl and K. Ramirez-Amaro, "Why did i fail? a causal-based method to find explanations for robot failures," *IEEE Robotics and Automation Letters*, vol. 7, pp. 8925–8932, 2022.
- [14] M. Diehl and K. Ramirez-Amaro, "A causal-based approach to explain, predict and prevent failures in robotic tasks," *Robotics and Autonomous Systems*, vol. 162, p. 104376, 2023.
- [15] O. Ahmed, F. Träuble, A. Goyal, A. Neitz, M. Wüthrich, Y. Bengio, B. Schölkopf, and S. Bauer, "Causalworld: A robotic manipulation benchmark for causal structure and transfer learning," 2020.
- [16] E. Bingham, J. P. Chen, M. Jankowiak, F. Obermeyer, N. Pradhan, T. Karaletsos, R. Singh, P. Szerlip, P. Horsfall, and N. D. Goodman, "Pyro: Deep universal probabilistic programming," *Journal of Machine Learning Research*, vol. 20, 2019.
- [17] R. Cannizzaro and L. Kunze, "Car-despot: Causally-informed online pomdp planning for robots in confounded environments," in *IEEE/RSJ International Conference on Intelligent Robots and Systems*, 4 2023.
- [18] J. Pearl, *Causality: Models, reasoning, and inference, second edition*. Cambridge university press, 2009.
- [19] T. Gerstenberg, "What would have happened? counterfactuals, hypotheticals and causal judgements," *Philosophical Transactions of the Royal Society B: Biological Sciences*, vol. 377, 12 2022.
- [20] R. Cannizzaro, J. Routley, and L. Kunze, "Towards a causal probabilistic framework for prediction, action-selection & explanations for robot block-stacking tasks," in *IEEE/RSJ International Conference on Intelligent Robots and Systems (IROS) 2023 Workshop on Causality for Robotics*, 2023.
- [21] R. Cannizzaro, R. Howard, P. Lewinska, and L. Kunze, "Towards probabilistic causal discovery, inference & explanations for autonomous drones in mine surveying tasks," in *IEEE/RSJ International Conference on Intelligent Robots and Systems (IROS) 2023 Workshop on Causality for Robotics*, 2023.
- [22] L. Mösenlechner and M. Beetz, "Parameterizing actions to have the appropriate effects," in *2011 IEEE/RSJ International Conference on Intelligent Robots and Systems*, pp. 4141–4147, 2011.
- [23] L. Kunze and M. Beetz, "Envisioning the qualitative effects of robot manipulation actions using simulation-based projections," *Artificial Intelligence*, vol. 247, pp. 352–380, 2017. Special Issue on AI and Robotics.
- [24] M. Beetz, D. Jain, L. Mosenlechner, M. Tenorth, L. Kunze, N. Blodow, and D. Pangercic, "Cognition-enabled autonomous robot control for the realization of home chore task intelligence," *Proceedings of the IEEE*, vol. 100, no. 8, pp. 2454–2471, 2012.
- [25] J. Pearl and D. Mackenzie, *The book of why: the new science of cause and effect*. Basic books, 2018.
- [26] E. Coumans and Y. Bai, "Pybullet, a python module for physics simulation for games, robotics and machine learning," 2016. <http://pybullet.org>, accessed 2024-03-15.
- [27] Toyota Motor Corporation, "Human support robot (hsr)," n.d. <https://mag.toyota.co.uk/toyota-human-support-robot>, accessed 2024-03-15.
- [28] N. Koenig and A. Howard, "Design and use paradigms for gazebo, an open-source multi-robot simulator," in *2004 IEEE/RSJ International Conference on Intelligent Robots and Systems (IROS) (IEEE Cat. No.04CH37566)*, pp. 2149–2154 vol.3, IEEE, 2004.
- [29] S. Garrido-Jurado, R. Muñoz-Salinas, F. J. Madrid-Cuevas, and M. J. Marín-Jiménez, "Automatic generation and detection of highly reliable fiducial markers under occlusion," *Pattern Recognition*, vol. 47, no. 6, pp. 2280–2292, 2014.
- [30] D. Coleman, I. A. Sucas, S. Chitta, and N. Correll, "Reducing the barrier to entry of complex robotic software: a moveit! case study," *Journal of Software Engineering for Robotics*, vol. 5, pp. 3–16, May 2014.